Design: Results of 50 patients that all utilized culture with acid fast (AF) stained smear, histologic evaluation, and *Mycobacterium tuberculosis* complex (MTb) PCR from the same anatomical site were reviewed. The study period was from July 2003 to August 2006. The archived histologic H&E and AF stained slides were retrospectively reviewed and evaluated for type of inflammation and maximum quantity of AF bacilli (AFB) per 100x field. Available formalin-fixed, paraffin-embedded (FFPE) tissue from patients with at least one positive testing modality were further tested with a real time mycobacterial species PCR assay using meltcurves to distinguish mycobacterial species. A comparison of the methodologies was performed with culture as the gold standard.
Results: Of the 50 patients, 26 (52%) were positive by a least one testing method. On histology, 19 (83%) of these patients demonstrated caseating granulomatous inflammation. By culture, MTb 9) was the most common isolate, followed by *M. avium* complex (7), *M. xenopi* (3), *M. szulgai* (1) and *M. marinum* (1). MTb PCR was positive in 4 cases (sensitivity 44%; specificity 100%). The average AFB quantity for positive and negative MTb PCR was 74 and 1, respectively (p value = 0.0159). The mycobacterial species PCR successfully identified 7/12 nontuberculosis isolates from culture positive patients. Of these, the average AFB quantity for positive and negative mycobacterial species PCR was 85 and 4, respectively (p value = 0.0303).
Conclusions: Nucleic acid amplification testing is a quick and effective method for identifying mycobacterial infection. The utility of PCR on FFPE tissue is of limited value when AFB are scant or absent on histology. However, a PCR assay with the ability to distinguish species provides a greater clinical benefit. Mycobacterial culture remains the gold standard and is necessary for antibiotic sensitivity testing.

1236 Is the Volume of the Added Blood to the Blood Culture Bottles Adequate? A Cross-Sectional Study in a County Hospital

N Zarrin-Khameh, CE Stager. Baylor College of Medicine, Houston, TX.
Background: The optimal volume of the added blood to the BacT/Alert 3D, aerobic and anaerobic blood culture bottle is 8-10 ml.
Design: As part of the quality control study of the microbiology laboratory in our county hospital, we assessed whether the volume of the blood added to the blood culture bottles (BCB) is adequate. 140 consecutive BCB (6 pediatric, 65 aerobic, and 69 anaerobic) were selected. Since one milliliter of blood weighs approximately one gram, the weight of BCBs was used to estimate the volume. Each BCB was weighed with a Miltter AE 100 scale. The weights were recorded in decimals. The weight of the added blood volume was calculated by subtracting the weight of the BCB from a similar unused BCB.
Results: The minimum, maximum, mean and median weight of the BCBs were 0.16, 14.8, 4.53, and 4.37 mg, respectively. **86.43% of the BCBs had less than 6 ml blood, and 2.86% of the BCBs had more than 12 ml blood**.
Conclusions: This study shows that in our county hospital the volume of added blood to BCBs is below the recommended volume of 8-10 ml. Our results suggest that similar studies should be part of the quality control of microbiology laboratories.

1237 Evaluation of Bayer Versant HCV Genotype 2.0 (LiPA 2.0) Assay

Q Zhao, R Marrison, C Oates, J Dong. University of Texas Medical Branch, Galveston, TX.
Background: Accurate genotyping of hepatitis C virus (HCV) is essential in the clinical management and monitoring of HCV infections and is also critical in HCV epidemiology studies. Therefore, it is essential to evaluate and choose sensitive and specific HCV genotyping method.
Design: The study evaluated the performance characteristics of the newly developed Versant HCV Genotype 2.0 (LiPA 2.0) assay (Bayer HealthCare, Tarrytown, NJ). The assay uses sequences of both the 5' UTR and core regions to determine HCV genotypes and subgenotypes (1, 1a, 1b; 2, 2a, 2b; 3, 3a, 3b, 3c/d; 4, 4a, 4b, 4a/4c/4d; 5, 5a, 5b; 6, 6a, 6b, 6c, 6d). The LiPA 2.0 assay was compared with Abbott real-time PCR HCV genotyping method which isvcurrently used in our Molecular Diagnostic Laboratory. Discordant genotypes and subgenotypes were examined by sequencing.
Results: A total of 123 HCV positive plasma/serum samples including 114 patient samples and 9 samples from commercial HCV RNA Genotype Performance Panel (PHW202, BBI Diagnostics) were tested by both methods. Twelve of the 114 patient samples were HCV positive by both genotyping methods. While Versant LiPA 2.0 successfully genotyped these 12 samples as 1a (2 cases), 1b (8 cases), and 3a (2 cases), Abbott Real time PCR method failed to genotype these samples (reported as indeterminate). Versant LiPA 2.0 assay correctly genotyped all samples in the PHW202 panel while Abbott assay failed to genotype the 1b sample (typed as indeterminate). These "indeterminate" HCV samples accounted for the great majority of the discordance (14/18 = 77.8%) between these two methods. The assay sensitivity was examined using series dilutions of two previously genotyped 1a and 1b samples by both methods. Versant LiPA 2.0 genotyped both subtypes at 1600 IU/mL, whereas Abbott assay genotyped 1a at 1600 IU/mL, but failed to genotype 1b even when the HCV viral load was much higher (e.g., 5,000 IU/mL,).
Conclusions: Compare with Abbott real-time HCV genotype assay, Versant LiPA 2.0 showed higher degree of genotyping sensitivity for subtyping 1b. To our knowledge, this is the first time the sensitivity level of Versant LiPA 2.0 assay has been evaluated.

Kidney

1238 Lymphoid Cell Proliferation in Renal Transplants. Biologic and Diagnostic Implications

H Akgun, A Ozcan, M Chirala, J Zhai, SS Shen, LD Truong. The Methodist Hospital, Houston, TX; Weill Medical College of Cornell University, New York, NY; Baylor College of Medicine, Houston, TX; Erciyes University, Kayseri, Turkey; Gülhane Military Medical Academy & School of Medicine, Ankara, Turkey.
Background: The initiation site of alloimmunity during renal transplant rejection remains controversial. It is not clear whether the alloreaction develops in peripheral lymphoid organs with the effector cells being subsequently recruited to the target organs, or the entire process of alloreaction including antigen presentation, maturation and proliferation of the effector cells can happen within the transplanted kidneys. Evaluation of the proliferation of inflammatory cells within the transplanted kidneys and the involved cell types may provide further insight and may aid in the diagnosis of acute cellular rejection (ACR).
Design: Interstitial inflammatory cell proliferation was evaluated by immunostain for MIB-1 in 129 kidney specimens. Double immunostain was performed to determine the cell types, i.e., T cells , B cells, or macrophages, that underwent proliferation The results were correlated with clinical features.
Results: The percentage of inflammatory cells in proliferation was 25.7 ± 5.4 in ACR (n = 24), which was significantly higher than in normal kidney (0.4 ± 0.2, n = 8), acute tubular necrosis (1.2 ± 0.5, n = 8), chronic allograft nephropathy (CAN) (2.4 ± 0.6, n=20), and native kidneys with diverse diseases (n = 63, 9.2 ± 2.3). It was, however, comparable to that in CAN with significant intertitial inflammation (20.6 ± 3.9, n= 16). The percentage of T cells in proliferation was 16.1 ± 2.1 and 18.9 ± 2.0 in ACR with or without CAN, whereas those for B cells or macrophages were low (< 1.7%), regardless of diagnostic categories. All cases diagnosed as ACR in conjunction with a high rate of MIB-1 + inflammatory cells, including one with superimposing BK virus nephropathy and one with "borderline" features; and 9 out of 12 cases with CAN and significant interstitial inflammation in which superimposing ACR was diagnosed, in part due to a high rate of MIB-1 + inflammatory cells, responded well to antirejection therapy.
Conclusions: Proliferation of interstitial inflammatory cells can be readily detectable in renal tranplants with ACR and this involves predominantly T cells. These observations not only provide additional support for the controversial concept of *in situ* alloimmunization, but may also facilitate the diagnosis of ACR in problematic cases.

1239 Alpha Heavy Chain Deposition Disease: A Comparison of Its Clinicopathological Characteristics with Gamma and Mu Heavy Chain Deposition Disease

MP Alexander, GP Mendez, V Nosé, HG Rennke. Brigham and Women's Hospital, Harvard Medical School, Boston, MA.
Background: Heavy chain deposition disease (HCDD) is a rare monoclonal immunoglobulin disorder characterized by the production and deposition of immunoglobulin heavy chains without a light chain. The predominance of gamma HCDD with only two cases of alpha HCDD reported thus far, prompted this study in which we describe two additional unusual forms of alpha HCDD and summarize and compare the clinicopathological characteristics of all identified cases in the literature.
Design: The clinical presentation, laboratory data, and pathology of 24 patients with HCDD, inclusive of two of our cases were compiled.
Results: The results are summarized in the table below. Gamma is the predominant heavy chain subset. Most patients present in the fourth to fifth decade with impaired renal function, proteinuria, and hypertension. Hypocomplementemia is exclusive to the gamma subset. Definitive association with a plasma cell dyscrasia is seen in all cases of alpha HCDD and only a small proportion of Gamma HCDD. The patterns of injury are predominantly nodular sclerosing glomerulopathy, with a dominant crescentic pattern of injury in the alpha HCDD and a rare endocapillary proliferative pattern in gamma HCDD. Extra-renal deposition is noted, with two cases of cutis laxa, single case of deposition in liver and thyroid, and another with skeletal muscle involvement. We documented unique binding of alpha heavy chains to elastic fibers in the skin in one of our cases.
Conclusions: Alpha HCDD, although less frequent among the HCDD, is often characterized by a crescentic pattern of injury and an associated plasma cell dyscrasia. A unique complication in few cases of HCDD is cutis laxa, possibly a consequence of active inflammation and elastolysis in response to the binding of the heavy chain to elastic fibers.

Summary of clinicopathological characteristics

Clinical characteristics	Alpha HCDD (n=4)	Gamma HCDD (n=19)	Mu HCDD (n=1)
Age range (average)	29-78(55)	35-73(54.3)	63
M:F	3:1	2:3	0:1
Cutis laxa	1/4	0	0
Urticarial vasculitis	1/4	0	0
Hypertension	4/4	16/19	1/1
Nephrotic range	3/4	13/19	1/1
Hypocomplementemia	0	10/19	0
Myeloma	4/4	3/19	0
Hepatitis C positivity	1/4	5/19	0
Nodular sclerosis	3/4	17/19	1/4
Crescents	3/4	3/19	0
Extraskeletal deposition	skin	skin, muscle, thyroid,liver	0

1240 Alpha- Actinin -4 Defficient Mice Develop Focal and Segmental Glomerulosclerosis with Features of Collapsing Glomerulopathy

S Alwaheeb, JM Henderson, A Weins, SV Dandapani, MR Pollak. Brigham and Women's Hospital, Boston, MA; Brigham and Women's Hosptial/Harvard Institutes of Medicine, Boston, MA.

Background: An inherited, late-onset form of focal and segmental glomerulosclerosis (FSGS) with autosomal-dominant inheritance is caused by mutations in the actin-crosslinking protein ∝-actinin-4. Our group has generated two different tools for studying disease pathogenesis: knock-in "KI" mice expressing the disease- associated mutation, and knock out "KO" mice deficient in ∝-actinin-4. We performed a detailed morphologic analysis of kidneys obtained from the 2 mouse models at various ages.

Design: On a mixed background (C57B16/129SvJ1), mice from all genotypes were sacrificed from 1 to 99 weeks of age. Kidneys were harvested and processed for light and electron microscopic analysis. Glomerular pathology including global sclerosis,segmental sclerosis and collapsing glomerulpathy (CG) were expressed as a percentage of the total glomeruli. Interstitial fibrosis was expressed as a percentage of the total tubulointerstitium. Tubular injurious changes were given a score of 0 to 3. Electron microscopic features such as glomerular basement membrane (GBM)abnormalities, foot process effacement (FPE) and microvillous transformation were given a score of 0 to 4.

Results: Homozygous KI/KI and KO/KO mice develop progressive glomerular and tubulointerstitial fibrosis with aging, with features of CG and FSGS. Tubules show features of acute injury. Tubular cystic dilatation and proteinacous casts are also present. Ultrastructural changes in the form of GBM abnormalities and podocyte FPE were only present in the KI/KI and KO/KO mice. Ultrastructural changes are observed at 4 weeks of age in the KI/KI mice and light microscopic changes at 5.4 weeks. Both ultrastructural and light microscopic changes are present at 4 weeks in KO/KO mice. The wild type (WT/WT) and heterozygote mice (WT/KO, WT/KI) were normal on both light and electron microscopic evaluation at all ages.

Conclusions: Mutations in the ACTN 4 gene cause podocyte damage with morphologic features of CG only in KI/KI and KO/KO mice. Although the human disease is present in the heterozygous state, all the heterozygous mice had normal morphologic features. This suggests that other factors may contribute to this appearance in humans. Furthermore the findings of CG are novel in our project and suggest that derangements of actin cross-linking may contribute to the pathogenesis of CG.

1241 PG695 and Tacrolimus Act Synergistically To Improve Renal Allograft Survival in Monkeys

NG Chan, HT Sun, R Zhong, B Garcia, H Qian, H Yang, W Liu, M Moussa. University of Western Ontario, London, ON, Canada.

Background: Calcineurin inhibitors (CNI) such as tacrolimus have reduced the incidence of acute rejection in renal allografts but have not significantly improved mortality associated with chronic rejection and drug toxicity. Novel agents such as PG695, used to treat autoimmune diseases, inhibits IL-2 gene expression via a different signaling pathway. The combination of these drugs may allow for lower doses of CNI, thereby minimizing toxicity, while improving renal allograft survival. **Objective:** To determine if PG695 and a subtherapeutic dose of tacrolimus (FK) act synergistically to prevent renal allograft rejection in monkeys.

Design: MHC-mismatched renal allografts were transplanted into twenty-four cynomolgus monkeys after bilateral nephrectomy. Recipients were randomly divided into the following groups: (i) no treatment; (ii) PG695 (0.06 mg/kg); (iii) PG695 (0.08 mg/kg); (iv) PG695 (0.1 mg/kg); (v) FK (1mg/kg); (vi) PG695 (0.04mg/kg + FK 1mg/kg); (vii) PG695 (0.06 mg/kg + FK 1mg/kg); (viii) PG695 (0.08 mg/kg + FK 1mg/kg). Recipients were sacrificed when serum creatinine exceeded 800 µmol/L or at a maximum of 100 days. Their kidneys were assessed according to the Banff 1997 Diagnostic Categories for Renal Allograft Biopsies.

Results: Animals receiving only PG695 (groups ii-iv) lived an average of 13 - 26 days and died of acute cellular or humoral rejection. Animals receiving FK only (group v) survived an average of 27 days and died of acute cellular rejection. Animals receiving a combination of PG695 and FK (groups vi-viii) lived an average of 57 - 68 days. Analysis of their kidneys showed acute tubular necrosis, atrophy and fibrosis, or borderline changes for rejection. Animals receiving no drugs (group i) lived an average of 7 days and had kidneys with features positive for acute cellular rejection.

Conclusions: Our findings show that combining a subtherapeutic dose of the classic drug tacrolimus with the novel agent PGP695 acts synergistically in improving renal allograft survival.

1242 The Potential Roles of Interstitial Plasma Cells (PC) and Ectopic Germinal Centers (GC) in Human Lupus Nephritis (LN)

A Chang, N Liu, SG Henderson, R Guttikonda, SM Meehan, MR Clark. University of Chicago, Chicago, IL.

Background: Immunophenotypic characterization of interstitial inflammatory cells in renal biopsies of lupus patients has previously focused on T cells. We hypothesized that interstitial PCs and ectopic GC formation in LN kidneys may play a significant role in the local production of pathogenic autoantibodies, such as those to native DNA.

Design: Standard immunohistochemistry was performed on paraffin tissue sections from 55 human LN biopsies using monoclonal antibodies to CD3, CD20, CD45, CD138, and MUM1. Glomerular lesions consisted of ISN/RPS classes II (4), III (16), IV (26), and V (9). Based on CD45, the interstitial inflammatory infiltrate was categorized into the following patterns: diffuse, B/T cell aggregates, and ectopic GCs. The percentage of $CD45^+$ cells staining for CD3, CD20, CD138, and MUM1 was assessed. CD21 was used in select cases to confirm the presence of follicular dendritic cell networks in GCs.

Results:

Interstitial inflammatory cell immunophenotype

Class	CD3+	CD20+	CD138+	MUM1+	# Cases
II	71.9%	11.7%	**9.5%**	6.7%	4
III	65.3%	12.1%	**13.5%**	16.6%	16
IV	66.2%	10.9%	**17.3%**	20.4%	26
V	68.3%	10.4%	**12.1%**	14.1%	9

Immunophenotype by inflammatory infiltrative pattern

Pattern	CD3+	CD20+	CD138+	# Cases
Diffuse	70.3%	**6.5%**	12.6%	30
B/T cell aggregates	62.9%	**15.9%**	17.2%	22
Ectopic GC	59.3%	**26.3%**	17.4%	3

$CD3^+$ T cells predominated, representing 67% of the total $CD45^+$ cells. $CD20^+$ B cells, $CD138^+$ PCs, and $MUM1^+$ post-GC B cells comprised 11%, 15% and 17%, respectively, of all $CD45^+$ cells. $CD20^+$ B cells and $CD138^+$ PCs were present in all biopsies, although biopsies with higher numbers of PCs tended to have fewer B cells. In 22 (40%) biopsies, >30% of the $CD45^+$ cells were of B cell lineage ($CD20^+$ or $CD138^+$ and/or $MUM1^+$). All 3 biopsies with GCs showed class V LN of which 2 had concurrent class III LN. When comparing different LN subclasses, there was a trend towards a higher percentage of PCs with class III and IV LN. Increased activity and chronicity indices correlated with statistically significant higher percentages of PCs and B cells, respectively.

Conclusions: B and PCs are present in significant quantities within LN kidneys, in a location to contribute to the pathogenesis of this autoantibody-mediated disease. The presence of ectopic GCs in a subset of LN biopsies is a novel finding which suggests that some lupus autoantibodies may be specifically targeting native renal antigens.

1243 Regulatory T Cells in Human Lupus Nephritis

A Chang, N Liu, SG Henderson, R Guttikonda, SM Meehan, MR Clark. University of Chicago, Chicago, IL.

Background: The number of circulating regulatory T cells (Tregs) in peripheral blood has been shown to inversely correlate with disease activity in patients with systemic lupus erythematosus. We hypothesized that a similar relationship might exist between the number of Tregs and disease activity in lupus nephritis (LN) renal biopsies.

Design: 30 human LN biopsies were studied. Glomerular involvement consisted of ISN/RPS classes II (2), III (8), IV (15), and V (5). Standard immunohistochemistry was performed on paraffin tissue sections using monoclonal antibodies to CD3, CD45, and Foxp3 (Treg transcription factor). Based on CD45 staining, the extent of interstitial inflammation was categorized as follows: <10%, 11-25%, 26-50%, and >50%. The histologic pattern of interstitial inflammation was also classified as follows: diffuse, B/T cell aggregates, or ectopic germinal center formation. The percentage of CD45+ and CD3+ cells staining for Foxp3 was manually counted and calculated. The percentages of Foxp3+ Tregs were compared with LN subclass, activity and chronicity indices, and other histopathologic features.

Results:

Percentage of Interstitial Treg by LN Subclass

LN Class	Foxp3+/CD3+	Foxp3+/CD45+	# Cases
II	0.5%	0.3%	2
III	3.8%	1.7%	8
IV	5.0%	2.7%	15
V	2.9%	1.7%	5

Percentage of Interstitial Tregs by Extent of Inflammation

Int inflamm	Foxp3+/CD3+	Foxp3+/CD45+	Cases
<10%	1.9%	0.5%	3
11-25%	4.1%	2.1%	8
26-50%	2.8%	1.6%	10
>50%	6.0%	3.1%	9

On average, CD3+ T cells represented 63.9% of the total CD45+ cells (range = 36.3-94.5%). The Tregs comprised a small percentage of the CD45+ interstitial lymphocytes (average = 2.1%, range = 0-10.2%) and CD3+ T cells (average = 4.1%, range = 0-23.7%). No significant differences were noted in the distribution of T cells or Tregs when comparing different subclasses of lupus nephritis. There was also no statistically significant correlation when comparing the percentage of Tregs with either the activity or chronicity indices, severity of interstitial inflammation, or histologic pattern of interstitial inflammation.

Conclusions: The percentage of interstitial Tregs in renal biopsies did not demonstrate significant correlation with the different subclasses, activity/chronicity indices, or other histopathologic features of LN.

1244 De Novo Focal Segmental Glomerulosclerosis with Collapse Associated with Sirolimus Therapy

LD Cornell, AB Collins, MK Selig, P Della Pelle, RB Colvin. Massachusetts General Hospital, Boston, MA.

Background: Proteinuria is recognized as a frequent, potentially adverse effect of sirolimus (rapamycin), commonly used as rescue therapy for renal transplant recipients who develop chronic calcineurin inhibitor toxicity. Sirolimus is an immunosuppressive and anti-proliferative drug that inhibits the mammalian target of rapamycin (TORi). In one study, up to 46% of patients developed proteinuria over 3-24 months after conversion to sirolimus. The pathogenesis of the proteinuria is controversial: the few reported cases with biopsies have provided evidence for tubular proteinuria, pre-existing or recurrent renal disease, and collapsing glomerulopathy.

Design: The renal biopsy and transplant databases at our institution were searched for patients who underwent renal transplantation between 11/2000 and 9/2004 and who began sirolimus therapy within three months after renal transplantation. Renal biopsies from these patients were examined by light, immunofluorescence, and electron microscopy.

Results: Twenty-five patients were identified who initiated sirolimus therapy within the first 3 months of renal transplantation. Ten of these patients underwent a total of 16 renal biopsies. Four biopsies from two patients were protocol biopsies; the others were indication biopsies. Of these 10 patients, two developed de novo focal segmental glomerulosclerosis (FSGS). One patient had been exposed to sirolimus for 16 months and had taken tacrolimus for the first 2 months post-transplant. The other patient had taken sirolimus and tacrolimus concurrently for 11.5 months. Both cases showed classic FSGS lesions with adhesions; one showed a collapsed glomerulus. Electron microscopy on both cases showed segmental GBM wrinkling with widespread, segmental podocyte foot process effacement and podocyte hypertrophy. Immunofluorescence microscopy showed staining for albumin in tubular reabsorption droplets and no glomerular deposits. No lesions of chronic calcineurin inhibitor toxicity or other causes of FSGS were identified in the two cases.

Conclusions: In this small series, FSGS was found in 8% of patients started on sirolimus in conjunction with other drugs. In neither case could the lesions be attributed to calcineurin inhibitor toxicity or pre-existing or recurrent disease. Podocyte lesions were clearly evident, in one case with collapse, suggesting that podocytes are affected by the drug. The mechanism is unknown but may involve known inhibitory effects of TORi on cell survival mechanisms (AKT pathway) or VEGF production.

1245 Non-Neoplastic Renal Lesions Are Often Unrecognized: A Review of 248 Adult Tumor Nephrectomy Specimens

KJ Henriksen, SM Meehan, A Chang. The University of Chicago, Chicago, IL.

Background: The pathologic evaluation of tumor nephrectomy specimens primarily focuses on the diagnosis, grading, and staging of the neoplasm. The presence of coincidental non-neoplastic pathologic changes in these specimens may have significant clinical implications for subsequent patient management. The purpose of this study is to determine the incidence and spectrum of non-neoplastic disease processes that are overlooked in tumor nephrectomies.

Design: We reviewed the H&E slides of 248 partial or total adult tumor nephrectomy specimens from our pathology archives between 1997 and 2002 with an emphasis on the non-neoplastic renal parenchyma. Analysis of specimens with significant pathology involving the non-neoplastic renal parenchyma included additional stains (periodic acid-Schiff and Congo red) and direct immunofluorescence microscopy performed on the paraffin sections for IgG, IgA and kappa and lambda light chains. The surgical pathology reports were reviewed to determine whether the non-neoplastic lesions were originally identified.

Results: After review of the H&E slides, 43 cases (17.3%) demonstrated suspicious alterations, such as diffuse and/or nodular mesangial sclerosis, mesangial hypercellularity, or glomerular basement membrane thickening, in the non-neoplastic parenchyma that warranted further study. Congo red stains and immunofluorescence microscopy were negative in these cases. After evaluation of the special stains and clinical correlation, the pathological changes in 24 cases were categorized as follows: diabetic nephropathy (severe-11 cases, and mild to moderate-10 cases), sickle cell nephropathy with focal segmental glomerulosclerosis (1 case), atheroembolic disease (1 case), and thrombotic microangiopathy (1 case). 21 (88%) of these diagnoses were missed during the initial pathologic evaluation. Only 3 severe diabetic nephropathy diagnoses (12%) were originally reported. Other pathologic features including varying degrees of global glomerulosclerosis, interstitial fibrosis, tubular atrophy, and arteriosclerosis were considered non-specific findings in this study.

Conclusions: Although accurate pathologic evaluation of renal neoplasms remains essential, the surgical pathologist should be aware that coincidental non-neoplastic renal diseases are commonplace and often not recognized, which may result in suboptimal patient care.

1246 Endogenous Lipocalin 2 Is Upregulated in Renal Tubulo-Interstitial Disease but Does Not Protect Against Cisplatin-Induced Nephrotoxic Injury

A Kats, J Kowaleska, RF Nicosia, CE Alpers, KD Smith. University of Washington, Seattle, WA.

Background: Lipocalin 2 (LCN2) is a siderophore binding protein that prevents enterobactin-dependent iron acquisition by enteric bacteria. LCN2 is constitutively expressed in neutrophil granules, and LCN2 expression is induced in many other cell types, including epithelial cells and mononuclear phagocytes. In addition to its role in host defense, LCN2 binds putative endogenous siderophores and is postulated to form an alternative iron acquisition pathway that is important for kidney development and the protection of renal tubular epithelial cells from ischemic and toxic injuries.

Design: We stained paraffin-embedded tissues from human kidney biopsies with anti-sera to LCN2. We tested a model of cisplatin-induced nephrotoxicity in wild type (WT) C57BL/6 mice, and LCN2-deficient mice.

Results: LCN2 is upregulated in renal tubular epithelial cells from biopsies with clinical and pathologic diagnosis of acute tubular necrosis/acute tubular injury. Increased expression of LCN2 is also present in biopsies from patient with acute pyelonephritis, where LCN2 localizes predominantly to infiltrating neutrophils. Cisplatin-treated WT mice upregulated LCN2 expression in their kidneys. However, cisplatin-treated WT and LCN2-deficient mice did not significantly differ in serum creatinine, blood urea nitrogen, or histologic scores of renal tubular epithelial cell injury.

Conclusions: LCN2 is upregulated in different forms of renal tubulo-interstitial disease, and the detection of LCN2 by immunohistochemistry provides a novel means for immunohistochemical assessment of renal tubular epithelial cell injury. Although LCN2 is upregulated in the setting of ischemic and toxic injury, endogenous LCN2 does not protect against cisplatin-induced nephrotoxicity. In agreement with this finding, a recently published study did not demonstrate a role for endogenous LCN2 in protection against ischemic nephropathy. Our data suggest that LCN2 is upregulated in several forms of renal interstitial injury, where it bolsters host defense barriers and acts as part of the host response to prevent bacterial infections.

1247 Mesangial Matrix Is Influenced by Glomerulopathic Light Chains

J Keeling, GA Herrera. Saint Louis University, St. Louis, MO.

Background: Normal mesangial matrix is composed of different proteins of which collagen IV is the main component. Cellular integrity is maintained by the matrix and they in turn modulate the matrix. Interaction of human mesangial cells (HMCs) with glomerulopathic light chains (GLCs) initiate cellular changes resulting in diverse glomerulopathies. The purpose of this research is to investigate the features of light chain-mediated glomerulopathies (light chain deposition disease [LCDD], AL-amyloidosis [AL-Am]) relating to the GLCs.

Design: 5 mm thick renal tissue fixed in formalin and embedded in paraffin were obtained from LCDD, AL-Am and normal post mortem kidneys and renal biopsies . H&E, Jones methenamine silver, Congo red stains and Immunohistochemistry to identify collagen IV and tenascin proteins were performed on these tissues. HMCs were grown on glass slides and treated with GLCs and culture medium serving as control. Cells and conditioned media were harvested at time points up to 96 hours. Cells were analyzed for tenascin and collagen IV expressions by immunohistochemistry, while conditioned media was analyzed for tenascin expression using an ELISA technique.

Results: Immunohistochemistry on glomeruli from renal tissue with LCDD showed greater quantities of matrix proteins compared to normal and AL-Am glomeruli. Amyloid deposits were noted in glomeruli from AL-Am tissue. Collagen IV and tenascin expressions were increased in the LCDD compared to AL-Am and control glomeruli. HMCs expressed higher amounts of tenascin in LCDD than AL-Am, while AL-Am treated cells showed higher amounts of collagen IV compared to LCDD and control. Tenascin expression was also higher in the conditioned media form LCDD than AL-Am and control. Increase was also time dependent.

Conclusions: Initial exposure of HMCs to GLCs results in cell proliferation which continues in LCDD but not in AL-Am. Increased expression of matrix proteins is evident in LCDDand contributes to the formation of nodules, while ECM is lost in AL-Am and amyloid accumulates. GLCs do influence the composition of the mesangial matrix.

1248 Patterns of Glomerular Injury in Kidneys Infiltrated by Lymphoplasmacytic Neoplasms

J Kowalewska, A Kats, KD Smith, CE Alpers, RF Nicosia. University of Washington, Seattle, WA.

Background: Glomerular injury may occur as a result of immune dysfunction in patients with remote lymphoplasmacytic neoplasms. Glomerular injury concurrent with direct infiltration of the kidney by lymphoplasmacytic neoplasms is a rare occurrence and has not been fully characterized.

Design: We reviewed all native renal biopsies received at the University of Washington from January 2002 through September 2006 all for evaluation of renal dysfunction, that were additionally evaluated by immunohistochemistry for possible lymphoplasmacytic disorder. We identified 15 patients, including 9 with proteinuria and 8 presenting with acute renal failure.

Results: The 15 renal biopsies that showed direct involvement of kidney by lymphoplasmacytic neoplasm consisted of 2 cases of multiple myeloma and 13 cases of B-cell neoplasms including diffuse large B cell lymphoma (n=3), chronic leukocytic leukemia/small lymphocytic lymphoma (n=6), and B-cell lymphomas that were not further characterized in the biopsy (n=4). Nine (60%) cases showed coexistent glomerular pathology including 6 biopsies with deposition of immune reactants: membranoproliferative glomerulonephritis (MPGN, n=4), membranous glomerulonephritis (MGN, n=1), and 1 case of lambda light chain amyloidosis; and 3 cases with minimal change disease (MCD). Additionally, 1 biopsy revealed concurrent diabetic nephropathy, and 2 showed ischemic glomerulopathy. In 2 cases the glomeruli were without significant pathologic abnormalities. In one case there were no glomeruli. In 6 cases the diagnosis of lymphoproliferative disease was first made on the kidney biopsy. Biopsies with MPGN, showed deposition of monoclonal IgM kappa (n=2), IgG kappa (n=1), or polyclonal IgG/IgM (n=1). The immune deposits were polyclonal in the case of MGN.

Conclusions: Lymphoproliferative disorders may be first diagnosed in renal biopsies performed for evaluation of renal dysfunction with or without proteinuria. Concurrent glomerular injury may be a direct result of the lymphoplasmacytic disorder, resulting in amyloid or monoclonal immunoglobulin deposition disease, or potentially may be caused indirectly, as in the cases of MCD and MGN.

1249 PAX2 Expression in Renal Dysplasia of Children and Adults

YH Lee, SW Hong, WH Jung, HJ Jeong. Yonsei University, College of Medicine, Seoul, Korea.

Background: Renal dysplasia is an abnormal development of the kidney, and is histologically characterized by the presence of primitive ducts, undifferentiated mesenchyme, and metaplastic cartilage. It is usually detected in childhood along with other urinary tract anomalies, however, it can remain unnoticed until adulthood. The pathogenesis of renal dysplasia has not been clearly established so far. Recently, molecular biologic studies have demonstrated that PAX2 gene mutation plays a major role in its development. This study was aimed to examine PAX2 expression and histologic differences in dysplastic kidneys of both children and adults.

Design: A total of 30 cases (10 adults and 20 children), diagnosed as renal dysplasia by nephrectomy, were the subject of the study. Histologic examination was performed using paraffin-embedded hematoxylin-eosin stained sections. PAX2 expression was evaluated using immunohistochemistry. Apoptosis was detected by Apop Tag detection kit. Each two cases of normal fetal kidneys and adult kidneys served as controls.

Results: In normal fetal and adult kidneys, PAX2 protein was strongly expressed in the subcapsular nephrogenic zone, and decreased down to the center with maturation. PAX2 was also strongly expressed in the epithelia of distal tubules and collecting ducts, but not in the mature podocytes and proximal tubules. In dysplastic kidneys, PAX2 showed a strong expression in epithelia of primitive ducts of both children and adults, but its

degree showed a significant decrease in adults compared to those of children (P=0.007). The mesenchyme surrounding the primitive ducts of children, however, showed stronger staining to smooth muscle actin antibody and trichrome stain compared to that of adults. Apoptosis tended to be more prominent in the undifferentiated mesenchyme than in the primitive duct epithelia of both adults and children. Apoptosis index was significantly higher in primitive duct epithelia than that of the surrounding normal collecting duct epithelia (P=0.000).

Conclusions: PAX2 is overexpressed in the primitive ducts of renal dysplasia, which is sustained until adulthood and associated with increased apoptosis. However, a decrease of PAX2 expression in dysplastic epithelia and less fibromuscular staining of mesenchymal cuff of adults may suggest a gradual regression of dysplastic elements with time.

1250 Pathologic Changes in Renal Allografts Associated with Foscarnet Therapy

SM Meehan, PV Kadambi, I Tang, A Chang. University of Chicago, Chicago, IL.

Background: Foscarnet (phosphonoformate), an inhibitor of viral DNA polymerase, may be used as therapy for cytomegalovirus (CMV) infection. Foscarnet crystallization and tubulointerstitial nephritis have been associated with use of this agent. This study describes pathologic lesions in renal allografts associated with foscarnet therapy.

Design: Fifteen renal allograft biopsies from 4 patients were evaluated by light microscopy, immunohistochemistry and in selected cases, by electron microscopy. Intravenous infusions of foscarnet (45-120mg/kg, 1-2 times daily, depending on GFR) were given for periods of 2 to 17 weeks. Seven biopsies were obtained prior to exposure to foscarnet. Four biopsies were obtained during the period of treatment and 4 were obtained 6 weeks to 8 months after cessation of therapy.

Results: Biopsies obtained during treatment had tubular epithelial nuclear enlargement, irregular nuclear contours, large irregular nucleoli, vesicular nuclear chromatin and cytoplasmic clefts. Viral inclusions were not identified. Immunohistochemical stains for CMV, polyoma virus (SV40-T antigen), and herpes simplex viruses I and II were negative. Viral particles were undetectable by electron microscopy. These nuclear features were identified in proximal and in distal tubules. The interstitium had edema with mononuclear, plasmacytic and polymorphonuclear infiltrates, and granulomas in one biopsy. Tubular nuclear atypia persisted for up to 8 months after cessation of therapy. Biopsies obtained prior to foscarnet therapy had no nuclear atypia. Crystalline deposits were not observed.

Conclusions: We report novel tubular epithelial nuclear reactive changes associated with exposure to foscarnet. These changes may mimic viral infection and may be associated with neutrophilic, plasmacytic or granulomatous interstitial nephritis.

1251 Paraprotein Deposition in the Kidney with Unusual Subepithelial Deposits Mimicking Membranous Nephropathy

GP Mendez, MP Alexander, HG Rennke. Brigham and Women's Hospital, Harvard Medical School, Boston, MA.

Background: Paraprotein deposition diseases of the kidney have variable and often unexpected clinical and morphologic presentations. The kidney complication can antedate the diagnosis of a B-cell disorder or the detection of a MGUS. Monoclonal immunoglobulin deposition (MID), the least frequent of the common complications of paraproteinemias, most often presents as a membranoproliferative glomerulonephritis; a membranous variant is a distinctly uncommon pattern of renal involvement.

Design: Four cases of MID with a membranous pattern of deposition were identified among all biopsies received during a 2-year period at our institution. The pattern of glomerular injury, isotype of the immunoglobulin deposited, and ultrastructural characteristics of the deposits were evaluated and recorded. The information on pertinent laboratory tests and clinical presentation was also obtained.

Results: Among a total of 32 cases of MID only four cases (12.5%) had a membranous pattern. The light microscopy features are indistinguishable from idiopathic membranous nephropathy. One case also showed segmental endocapillary proliferation, and overt cortical infiltration by monotypic B-cells. The immunofluorescence microscopy showed strong reactivity for IgG along the peripheral capillaries. Three cases had an IgG/kappa-restricted profile and one case showed an IgG/lambda isotype. By electron microscopy, all cases showed subepithelial electron dense deposits; two cases showed organized, parallel, curved microtubular substructures with an average diameter of 15 and 20 nm and in two cases the substructures were ill-defined, with short, curved micro-fibrillary arrays. Other concurrent complications of paraproteins were not detected in these four biopsies. The clinical presentation was significant for heavy proteinuria (average >4.5 g/24 h); one case had myeloma, one patient was diagnosed with B-cell lymphoma after the kidney biopsy, and one case showed a circulating IgM/lambda, with negative bone marrow or lymphatic work-up.

Conclusions: Membranous glomerulopathy can represent the morphological expression of a paraprotein deposition in the kidney, and only immunofluorescence microscopy with light chain-specific reagents and the electron microscopy examination allow a consistent identification of such cases. This unusual pattern of deposition probably relates to unique physicochemical characteristics of the paraprotein or an antibody-like specificity for some component of the lamina rara externa or the cell membrane of the podocyte.

1252 Parietal Podocytes in Human Donor Kidney Biopsies Do Not Correlate with Donor Age

AK Miller, IW Gibson. University of Manitoba, Winnipeg, MB, Canada.

Background: Visceral podocytes cover the glomerular capillary tuft, functioning in filtering of plasma into Bowman's space. Previous studies have demonstrated that, in the majority of human glomeruli, podocytes also extend onto Bowman's capsule (BC) around the vascular pole; referred to as parietal podocytes. These studies have identified parietal podocytes in the normal kidney of tumour nephrectomies, predominantly from an elderly population. The aim of this study was to investigate parietal podocytes in normal human kidney from a younger population, to determine if their presence and extent correlate with age.

Design: We studied 65 implantation (time zero) kidney biopsies from donors within the age range of 10-69 years, with a sample of between 8 and 14 biopsies from each of the six decades. Biopsies were stained for podocyte immunocytochemical markers GLEPP-1 and synaptopodin. For each glomerulus, the percent of BC showing podocyte labelling was graded, as follows: 0 = 0%, 1 = <25%, 2 = 25-49%, 3 = 50-74%, 4 = 75-99%, 5 = 100%).

Results: Parietal podocytes were found at all age groups, in overall approximately 50% of glomeruli, as shown in the table below. They were present around the vascular pole area, most commonly lining <25% of BC, and were sometimes associated with podocytic connections between the capillary tuft and BC. There was no statistical correlation between presence or extent of parietal podocytes and donor age. In donors over 20 years of age, occasional glomeruli (<3%) showed 100% of BC lined by parietal podocytes. They had contracted capillary tufts, and cystic expansion of Bowman's space with proteinaceous material containing variable numbers of detached podocytes; features suggestive of atubular glomeruli.

Conclusions: These findings indicate that parietal podocytes are present in human kidney from all age groups, and are not merely a consequence of aging. The functional significance of parietal podocytes in human kidney warrants further investigation.

Parietal podocyte staining

Age Group	n	% glomeruli with parietal podocytes (GLEPP)	% glomeruli with parietal podocytes (Synaptopodin)	Mean grade of parietal podocytes (GLEPP)	Mean grade of parietal podocytes (Synaptopodin)
10-19	8	30.9	25.4	0.29	0.58
20-29	11	60.1	48.4	0.82	0.57
30-39	11	60.7	40.2	0.70	0.47
40-49	13	71.7	49.6	0.97	0.58
50-59	14	56.3	45.6	0.75	0.62
60-69	8	52.3	65.4	0.67	0.97

n = number of biopsies

1253 Incidence and Prognostic Value of CD20 Positive B-Lymphocyte Infiltrates in Renal Allograft Biopsies with Acute Cell Mediated Rejection

BS Mohammed, W Tsai, H Rahman, E Kraus, L Racusen, M Haas, S Bagnasco. Johns Hopkins University School of Medicine, Baltiomre, MD; Johns Hopkins University School of Medicine, Baltimore, MD.

Background: Association of B-lymphocyte infiltrates in kidney allograft biopsies with acute cell mediated rejection (AR), and poor response to treatment / increased risk of graft loss had been recently studied with variable results. These studies involved limited number of cases and included type 1 AR with only rare type 2 AR. No large study has been performed on such association in type 2 AR in the first year post transplant.

Design: We examined the frequency of B-lymphocytes infiltrates in renal allograft biopsies with AR (type 1 or type 2) detected by immunohistochemical stain for CD20. Most biopsies were stained for CD3 for T cells, some also for C4d. Positive cells for CD20 were counted by two pathologists blinded to the clinical background. Clinical information included serum creatinine prior to rejection, at rejection and at 1 , 3, 6 months, 1, 2, 3, 4 years after rejection; record of treatment, graft loss and death.

Results: Out of 220 biopsies performed from 1999 to 2001 at JHU and showing AR1 or AR2 within 1 year post transplant, 78 biopsies from 61 adult patients (age range: 22-75 Ys) had interstitial inflammation involving at least 25% of cortex and available clinical information. Exclusion criteria were: concurent functioning solid organ transplants, antibody mediated rejection, primary glomerular disease, viral infection, PTLD, and treatment with rituximab. Results are shown in (Table 1-1). Baseline immunosuppression for both AR1 and AR2 groups included prednisone +/- calcineurin inhibitors, mycophenolate and rapamycin. Rejection was treated with prednison in all patients +/- thymoglobulin and OKT3. Serum creatinine at rejection, at 1 month, and 1 year post biopsy was not significantly different between AR1 patients with B cell clusters of >100 or <100 cells.

Conclusions: Our data show that B-lymphocyte infiltrates are present in both AR1 and AR2, and suggest that these infiltrates may not be associated with worse response of AR1 to treatment.

	CD20, Negative	CD20, 20-50 cell/cluster	CD20, 50-100 cell/cluster	CD20, 100-200 cell/cluster	CD20, >200 cell/cluster
AR 1	13/40 (32.5%)	4/40 (10%)	6/40 (15%)	13/40 (32.5%)	4/40 (10%)
AR 2	13/38 (34%)	6/38 (16%)	5/38 (13%)	10/38 (26%)	4/38 (11%)

Table 1-1

1254 Immunofluorescence on Pronase-Digested Paraffin Sections: A Valuable Salvage Technique for Renal Biopsies

SH Nasr, SJ Galgano, GM Markowitz, MB Stokes, VD D'Agati. Columbia University, College of Physicians & Surgeons, New York, NY.

Background: Immunofluorescence (IF) on frozen tissue is the method of choice for the study of medical renal diseases. Not uncommonly, however, glomeruli are not present in the portion of the biopsy submitted for IF. In this case, formalin-fixed, paraffin-embedded tissue sections prepared from the portion of the biopsy allocated for light microscopy can be used as substrate for IF following antigen retrieval with proteases.

Design: We compare the sensitivity of immunofluorescence on frozen sections (IF-F) *versus* paraffin-embedded, pronase-treated sections (IF-P) for the detection of immune deposits in 63 renal biopsies from patients with various forms of medical renal disease.

Results: By using IF-P, diagnostic findings (based on the intensity and regularity of the distribution of staining) were obtained in 100% of cases of lupus nephritis (8/8 cases), acute postinfectious glomerulonephritis (3/3), cryoglobulinemic glomerulonephritis (3/3), fibrillary glomerulonephritis (3/3), primary amyloidosis (5/5), myeloma cast nephropathy (5/5), and light chain Fanconi syndrome (LCFS) (10/10) (Figure 1), 88% of cases of IgA nephropathy (7/8) (Figure 2), 80% of cases of light chain deposition disease (4/5), 50% of cases of idiopathic membranous glomerulopathy (MGN) (4/8), and 33% of cases of membranoproliferative glomerulonephritis type 1 (1/3) and anti-GBM disease (1/3). IF-P was less sensitive than IF-F for the detection of C3 in all disease categories and for the detection of IgG in cases of MGN and anti-GBM disease. The diagnostic kappa light chain staining was demonstrated in 100% (10/10) of cases of LCFS by IF-P vs. 40 % (4/10) by IF-F.

Conclusions: We conclude that IF-P is a valuable salvage immunohistochemical technique for renal biopsies lacking adequate cortical sampling for IF-F, and is superior to IF-F for the diagnosis of LCFS.

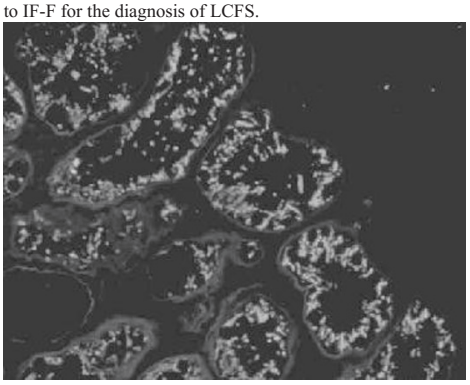

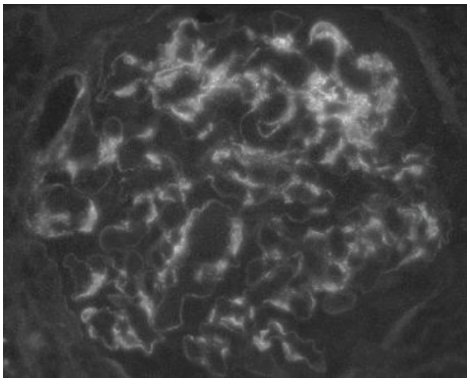

1255 Thin Basement Membrane Nephropathy Cannot Be Diagnosed in Deparaffinized, Formalin-Fixed Tissue

SH Nasr, GS Markowitz, AM Valeri, Z Yu, L Chen, VD D'Agati. Columbia University, College of Physicians & Surgeons, New York, NY.

Background: In diagnostic renal pathology, electron microscopy is ideally performed on glutaraldehyde-fixed, plastic resin-embedded tissue (EM-G). When no glomeruli are present in the portion of the biopsy fixed in glutaraldehyde, formalin-fixed, paraffin-embedded tissue can be reprocessed for electron microscopy (EM-F). This salvage technique is usually adequate for detection of many renal ultrastructural alterations such as the presence and site of electron-dense deposits and the degree of foot process effacement. The usefulness of this salvage technique for the diagnosis of thin basement membrane nephropathy (TBMN), a glomerular disease that can only be diagnosed by ultrastructural analysis, has not been studied systematically.

Design: we compared the glomerular basement membrane (GBM) thickness by EM-G versus EM-F in 21 renal biopsies, including TBMN (8 patients), normals (2 patients), minimal change disease (MCD) (6 patients), and diabetic nephropathy (DN) (5 patients). A minimum of 2 glomeruli were studied ultrastructurally by EM-F and by EM-G. GBM measurements were performed using a magnification graticule placed over the electron micrographs with final print magnifications of 2000 to 8000. For each biopsy, a total of 80 GBM measurements were made on EM-F and 80 measurements on EM-G. The measurements were performed at multiple representative points along randomly selected capillaries. The average (arithmetic mean) and standard deviation of the 80 measurements of each biopsy on EM-G and EM-F were then calculated.

Results: There was significant reduction of the GBM thickness by EM-F compared with EM-G across all diagnostic categories in all 21 cases. The mean percentage reduction in GBM thickness was 23% for the TBMN cases ($p = 0.004$), 40% for the normal/MCD cases ($p = 0.004$), and 34% for the DN cases ($p = 0.031$). Four patients with MCD had a mean GBM thickness by EM-F that fell below the defining threshold for diagnosis of TBMN. For the TBMN cases, the 99th percentile for GBM thickness by EM-F was 194 nm, suggesting that the diagnosis of TBM by EM-F can be excluded with confidence if the GBM thickness is above 200 nm. No clear criteria could be established to diagnose TBMN by EM-F.

Conclusions: Renal pathologists should be aware that reprocessing of paraffin tissue for EM causes artifactual GBM thinning that precludes accurate diagnosis of TBMN.

1256 Tubulo-Centric Granulomatous Interstitial Nephritis in Renal Allograft Recipients with Polyomavirus Nephropathy

V Nickeleit, D Thompson, M Latour, G Chan, H Singh. The University of North Carolina, Chapel Hill, NC.

Background: Granulomatous interstitial nephritides are very rare findings in renal allograft biopsies. Besides bacterial and fungal infections, allergic reactions to drugs, sarcoidosis, and productive adenovirus infections enter into the differential diagnosis. Granulomatous inflammation has so far not been reported in polyoma-BK-virus nephropathies (BKN).

Design: 26 patients with BKN were identified from the files; 4/26 patients demonstrated ill defined, non-necrotizing tubulo-centric granulomas that were small in 3/4 (patients 1-3) and large and progressive in 1/4 cases (patient 4). Morphologic and clinical data were analyzed.

Results: The formation of non-necrotizing granulomas, rich in histiocytes, was predominantly detected in and around markedly distended tubules with attenuated and focally ruptured basement membranes. The inflammatory response surrounded affected tubules in a cuff-like fashion. Immunohistochemistry demonstrated in some but not all granulomas in the central portion (representing the injured tubules) occasional expression of the polyomavirus T-antigen (in epithelial cells) and viral capsid proteins that were not detected in the interstitial inflammatory cell response. Adenovirus antigens, fungal or acid fast bacilli were not found. Standard immunofluorescence microscopy revealed granular complement C3 and C4d deposits along affected tubular basement membranes, however, immunoglobulins and light chains were not noted. In one case (patient 4) histiocytes containing rare intracytoplasmic and intralysosomal polyomaviruses were seen in the urine by electron microscopy. By PCR all patients showed high levels of BK-virus DNA in the urine (between $1x10^7$ and $5x10^9$ BK copies per ml). JC virus was only found in 2/4 patients; low sporadic JC shedding in one patient, and high, persistent JC shedding in patient 4 ($5x10^8$ copies per ml urine over 12 weeks). During further follow-up (2 - 8 months) patients 1-3 either cleared the virus from the graft (n=2) or viral replication stabilized at low levels (n=1). Patient 4 progressed to graft failure within 3 months.

Conclusions: We report for the first time the formation of granulomas in BKN that form in rare patients likely due to focal tubular rupture. It is tempting to speculate that the marked co-activation of JC viruses, the uptake of polyomaviruses into histiocytes, and/or the activation of complement factors along tubular basement membranes contribute to the formation of granulomas and graft failure in most severe cases.

1257 Thymosin β4 Is Increased in Renal Interstitial Fibrosis

D Orhan, EM Donnert, BJ Xu, A Gaspert, L-J Ma, AB Fogo. Hacettepe University Faculty of Medicine, Ankara, Turkey; Vanderbilt University Medical Center, Nashville, TN.

Background: We have previously shown that the G-actin sequestering protein thymosin β4 is a marker of early glomerulosclerosis. We now investigated whether thymosin β4 is increased in interstitial fibrosis.

Design: The unilateral ureteral obstruction (UUO) model in mice was used to induce tubulointerstitial fibrosis, and subgroups were treated with low or high dose antibody (Ab) to transforming growth factor (TGF)-β1. Morphological, immunohistochemical and biochemical investigations were performed at sacrifice at day 14, comparing to contralateral kidneys. Glomeruli and interstitial tissue from contralateral vs UUO kidneys were isolated by LCM, and protein profiles were acquired directly by MALDI-MS to assess for thymosin β4.

Results: Tubulointerstitial injury score was markedly increased in UUO, and not significantly changed by anti-TGF-β. Thymosin β4 immunostaining was markedly increased in all UUO mice versus contralateral kidneys (thymosin β4-positive cells/hpf 26.2±3.4 versus 0.5±0.6, $P< 0.0001$). Interstitial thymosin β4 was identified in macrophages, myofibroblasts, lymphocytes, and rare peritubular capillary endothelial cells (cells identified by morphology and immunohistochemistry for fibroblast specific protein-1 and F4/80). Rare tubular epithelial cells were positive for thymosin β4. Thymosin β4 was also increased in glomeruli from UUO vs contralateral kidneys, with increased positivity in high dose TGF-β Ab group, attributable mainly to increased podocyte staining ($P=0.02$ vs UUO and UUO+low dose TGF-β antibody). MALDI-MS showed increased thymosin β4 in interstitium in UUO compared to glomeruli.

Conclusions: TGF-β antibody did not significantly affect total UUO injury, but had a dose-dependent effect on podocyte thymosin β4 expression. We speculate that podocyte thymosin β4 positivity may reflect injury due to obstruction. We conclude that thymosin β4 is increased in a multiplicity of interstitial cells in the UUO model. Thymosin β4 may be a novel target for modulation of interstitial fibrosis.

1258 Typing of Amyloid Deposits in Surgical Pathology – Experience from a Single Laboratory with 110 Cases

MM Picken. Loyola University Medical Center, Maywood, IL.

Background: The treatment of systemic amyloidoses depends on the type of amyloid deposits. From a patient management point of view, diagnosis of systemic amyloidosis should be considered in three categories: amyloid derived from immunoglobulin light chain (AL), amyloid 2^0 to chronic inflammatory response (AA) and hereditary types. Current treatments are quite radical and include aggressive chemotherapy for AL, liver transplantation for hereditary types, and control of the underlying condition for AA; new amyloid-type specific therapies are also emerging. Thus amyloid typing is the current standard of care.

Design: Results of amyloid typing in 110 cases from a single laboratory were reviewed. For typing, a panel of antibodies was used: anti-amyloid P component, κ and λ light chain, AA amyloid protein, transthyretin and fibrinogen; in the setting of long term dialysis anti-$ß_2$-microglobulin was added. Stain for amyloid P (AP) component, which

is positive in all types of amyloid, served as a bulit-in positive control and a reference for intensity of stain. The intensity of stain was compared among the panel stains performed by the same technique, i.e. either in frozen (FS) or in paraffin (PS) sections. Interpretation of stains was made in conjunction with Congo red stain.
Results: There were 71 kidneys, 13 heart, 13 GI, 9 misc. specimens. Overall, typing of amyloid deposits was successful in 90% and 85% of cases respectively in FS and PS sections. In 13.6% of cases with inconclusive stains, AL was diagnosed based on collateral studies. The major amyloid types differed depending on tissue site, with AL, AA and ATTR diagnosed most frequently. At least one patient had combined deposits of ATTR/AL (confirmed by sequencing). A subset of AL is expected to be non-reactive with commercial antibodies due to truncation of the light chain. In such cases, the major differential diagnosis is between AL and hereditary types, and additional studies are required. Caution is advised in the interpretation of stains, and in distinguishing true from background stain. The use of a panel of antibodies is helpful in selecting the diagnostic stain which provides the strongest signal i.e. with an intensity that is comparable to the stain for AP.
Conclusions: With use of a panel of antibodies, unequivocal typing of amyloid can be achieved in the majority of cases, with results for FS better than for PS. The major challenge is diagnosis of AL with confidence. Although hereditary forms are rare, they are increasingly recognized. A single patient may suffer from different amyloid diseases simultaneously.

1259 Acutely Rejecting Human Renal Allografts but Not Well Functioning Grafts Are Infiltrated by FOXP3+ T Regulatory Cells

SV Seshan, D Dadhania, NL Seshan, B Li, T Muthukumar, R Ding, V Sharma, M Suthanthiran. Weill Medical College of Cornell University, New York, NY.
Background: A specialized subset of CD4+CD25+ T lymphocytes, termed regulatory T lymphocytes (Treg cells), is critical for suppressing autoimmunity and maintaining self-tolerance. Treg cells express FOXP3, which is a transcription factor that is induced by TGF-b. We reported that urinary cell FOXP3 mRNA levels are higher during acute rejection (AR) compared to those with stable graft function (Muthukumar et al. NEJM 2005). In experimental models, tolerant allografts are infiltrated by T regs. Thus, despite our findings of low urinary cell FOXP3 mRNA levels stable allografts, due to lack of tubulitis, the infiltrated FOXP3+ cells may fail enter the urinary space.
Design: We investigated the hypothesis that stable allografts are also infiltrated by FOXP3+ cells but these cells remain in the interstitial space. Paraffin embedded renal allograft biopsies from 28 recipients with confirmed AR and protocol biopsies from 22 recipients with stable function showing no AR, were stained with a polyclonal rabbit antibody to FOXP3 peptide (Abcam), using immunoperoxidase technique and Vision Biosystem detection systems. Nine allograft renal biopsies with biopsy proven AR and 12 biopsies without AR were analyzed for FOXP3 mRNA levels using kinetic quantitative PCR assay.
Results: The number of FOXP3 + cells were higher in 28 biopsies with AR compared to 22 biopsies without AR and the high levels were observed both as scattered infiltrates (33.5±4.2 cells/10HPF vs. 1.3±0.38 cells/10HPF, P<0.0001) or as tubular infiltrates (7.8±1.2 cells/10HPF vs. 0.1±0.1 cells/10HPF, P<0.0001). In the AR biopsies, a striking correlation between the FOXP3 scattered infiltrates and FOXP3 tubular infiltrates was observed (Spearman rank correlation r=0.75, P<0.0001). Intragraft FOXP3 mRNA levels were significantly higher in 9 allograft biopsies classified as AR compared to 12 biopsies without AR (P=0.006, Mann Whitney test).
Conclusions: Acutely rejecting human renal allografts, but not well functioning allografts, reveal marked infiltration by FOXP3+ cells. Unlike experimental tolerant allografts, the latter are not infiltrated by FOXP3+ cells. We suggest stable function of clinical allografts is more due to absence of graft destructive immunity rather due to the presence of graft adaptive immunity.

1260 A New Frontier for an Old Established Technique: Negative Staining Urine Electron Microscopy Is a Sensitive and Specific Noninvasive Tool To Diagnose Polyomavirus-BK-Nephropathy

HK Singh, V Madden, RK Detwiler, D Thompson, V Nickeleit. The University of North Carolina, Chapel Hill, NC.
Background: Polyomavirus-BK-Nephropathy (BKN) is a well known complication after renal transplantation. Noninvasive screening tools for identifying patients at risk for BKN include quantitation of decoy cells and quantitative urine and/or plasma PCR analyses, however, these tests lack specificity for accurately separating patients with BKN from asymptomatic viral activators. Negative staining urine electron microscopy (nsEM) is a well established but largely forgotten noninvasive tool that has been used for decades to search for viruses in various body fluid samples including urine. We report a retrospective analysis to determine if the detection of dense three dimensional polyomavirus clusters ("Haufen") by nsEM is a sensitive and specific technique to diagnose patients with BKN.
Design: 60 urines from 10 patients with biopsy proven BKN (2-11 samples/patient over 15 months followup)(Group A) and 48 urines from 25 control patients with signs of polyomavirus activation but no BKN (1-5 samples/patient over 14 months followup)(Group B) were analyzed.
Results: BKN, Group A) At time of initial biopsy diagnosis, 100% of patients showed shedding of "Haufen" by nsEM, urine decoy cells (median: 50, range = 10-150), and positive urine and plasma PCR viral load levels. During followup (median=9months; range=3-15 months), 7/10 patients overcame disease over 3-30 weeks with clearance of Haufen and decoy cells along with negative or markedly decreased urine and plasma viral load levels; 1/7 patients had a repeat kidney biopsy negative for BKN. 3/10 patients had persistent BKN with continuous shedding of Haufen, urine decoy cells, and positive urine and plasma viral load levels. Control Group B) No samples (n=48) showed "Haufen" by nsEM. All samples (n=48) showed urine decoy cells (median= 30; range =10-100). 19 samples from 5 patients showed persistent positive plasma PCR assays. Renal biopsies performed in these 5 patients did not show histologic evidence of BKN.
Conclusions: nsEM of urine to detect "Haufen" is a highly specific noninvasive diagnostic tool for identifying patients with BKN. Our data suggest a positive and negative predictive value for BKN of >95%. The pathologist can play a crucial clinical role with this new application of an old established diagnostic technique.

1261 The Anatomy of the Glomerular Diffuse Lesion (DL) in Diabetes

LC Stout, RE Lyon, EB Whorton. Univ TX Med Branch, Galveston, TX.
Background: Diabetic nephropathy is the major cause of renal insufficiency in the USA, and the diffuse lesion (DL) is the major cause of the mesangial matrix expansion (MME) that occludes the glomerulus (glom). Early stage DL, described in the 1970's, is a diffuse increase in MME during the first 5 years of Type I diabetes mellitus (T1DM). We and others assumed that a gradual progression of these early changes, visible only by electron microscopy (EM), led to the much larger MME's of late stage DL (LSDL), and thus concluded that the DL had a biochemical etiology. However, as far as we know the pathogenesis of LSDL has never been elucidated.
Design: 74 consecutively autopsied diabetic (D) and 59 matched control (C) cases were studied. A subset of 25 D and 12 C with the most diffuse and nodular MME's, ranging from mild to severe, but not end stage was studied intensively. PAS stained 4 micron step serial sections (25 D, 12 C) and 3 micron serial sections (2 D, 2C), plastic embedded 1 micron serial sections (2D, 2C), and 7 step serial section EM whole glom montages (1D) were studied in mostly Type II diabetic (T2DM) cases. The least and most DL were graded on a scale of 1 to 5 at 3 levels in about 100 gloms in each of 18 D and 8 C from the intensively studied cases, and at 1 level in 50 gloms per case in the remainder.
Results: Pure severe LSDL was uncommon, since many lesions >3 were nodules. DL lesions <3, termed intermediate stage DL (ISDL) exhibited considerable inter and intraglom variation in grade. In the 18 D cases, mean least and most DL were 0.53 (SD 0.13) and 2.07 (SD 0.58), respectively. Serial sections explained this variability, showing that ISDL was not diffuse, but by interposition completely encased the first and second order branches of the afferent arteriole (AA). In cross section these AA branches were identical to the well known "donut" lesions. As the process advanced, the gloms became partially lobulated due to obliteration of peripheral anastomoses. In one T1DM case with relatively severe DL an entire first order AA branch in 1 glom, and a peripheral capillary loop extending through 35 microns in another, were rendered atrophic and bloodless.
Conclusions: This peculiar distribution of MME suggests that ISDL forms in an attempt to throttle increased flow/pressure downstream from the AA, and thus may be due to a hemodynamic abnormality. It is hypothesized that MME extending beneath the endothelium compresses branch orifices, thereby eliminating relatively large segments of the glom tuft.

1262 Ex-Vivo Kidney Perfusion Model To Study Pathogenesis of Light Chain-Mediated Glomerulopathies

J Teng, N Galvin, GA Herrera. Saint Louis University Medical Center, Saint Louis, MO.
Background: The pathogenesis of light chain-mediated glomerulopathies has been studied using an in-vitro model which has provided insight into crucial steps in the development of two disease processes: light chain deposition disease (LCDD) and AL-amyloidosis (AL-Am). The present study aimed at the development of an animal model to determine whether the data obtained from the in-vitro model was reproducible, thus providing a platform to further study pathogenesis of these disorders and possible therapeutic interventions.
Design: The system used consisted of a perfusion chamber with constant temperature maintained at 37 °C and the pressure at the level of the renal artery at 120-150 mm Hg. Glomerulopathic light chains (G-LCs) purified from the urine of patients with renal biopsy-proven LCDD and AL-Am were diluted in perfusion media enriched with 95% O_2 and 5% CO_2 and perfused in isolated rat kidneys for up to 12 hours (n=8) . Urine samples were collected every 30 minutes for renal function tests and the arterial pressure and pH variations were monitored during the perfusion period. Kidney samples were obtained for immunofuorescence (IF) staining for kappa and lambda light chains (LCs) and ultrastructural evaluation, including immunogold labeling for LCs 3, 6 and 12 hours post-perfusion. Rat kidneys perfused with media alone were used as controls (n=4) .
Results: In kidneys perfused with AL-LCs, the process of clathrin-mediated LC internalization and delivery to mature lysosomal compartment was clearly visualized in transformed "macrophage-like" mesangial cells. Early amyloid deposition was identified focally in the mesangium. In kidneys perfused with LCDD-LCs the interaction with surface caveolin-like structures in mesangial cells, without significant internalization, was noted and early expansion of the mesangial matrix was identified focally. Ultrastructural labeling identified GLCs in the various cellular and extracellular compartments at different stages of the processes and the findings correlated with IF data derived from the same specimens. No alterations were noted in the control group.
Conclusions: The results obtained in this organ-based model corroborated data generated by the in-vitro model and the process of mesangial amyloidogenesis could be clearly delineated in vivo. This is an excellent model that can be used to test therapeutic interventions to try to prevent or ameliorate progression of renal damage in these patients.

1263 Renal Pathology in Hematopoeitic Cell Transplantation Recipients

ML Troxell, M Pilapil, D Miklos, JP Higgins, N Kambham. OHSU, Portland, OR; Stanford Univ, Stanford, CA.

Background: Hematopoietic cell transplantation (HCT) associated acute and chronic renal toxicity can be due to cytotoxic conditioning agents, radiation, infection, immunosuppressive agents, ischemia, and graft versus host disease (GVHD). We have reviewed consecutive renal biopsy specimens in HCT patients from a single center.

Design: The files of Stanford University Medical Center Department of Pathology were searched for renal biopsy specimens in patients who received HCT (1995-2005); 11 cases were identified (post BMT time 0.7 to 14.5 years). The biopsies were processed using standard techniques, and the findings were correlated with clinical data derived from medical records.

Results: The most common indication for HCT was a hematopoietic malignancy while one patient had stage IV breast carcinoma; 5 patients had autologous HCT using GCSF mobilized peripheral blood stem cells (PBSC), and 6 received HLA identical allogeneic PBSC transplants. Indications for renal biopsy included severe proteinuria (n=4), increased serum creatinine (n=4), or both (n=3). Findings on renal biopsy were variable, with many patients having more than one type of lesion. Membranous glomerulonephritis (MGN) was the most common diagnostic category (n=5), including 2 patients with autologous HCT and 3 with evidence of chronic GVHD elsewhere. 3 MGN patients achieved sustained remission with Rituximab therapy. Acute tubular necrosis (ATN) and/or tubulointerstitial nephritis was seen in 3 patients. Features of thrombotic microangiopathy (TMA) were present in the remaining 3 biopsies, including one attributable to calcineurin inhibitor toxicity. Of 10 patients with followup (2-64 months, median 14 months), 6 had chronic renal insufficiency, 1 had ESRD, and 3 had essentially normal renal function; only 2 had relapse of primary disease (one with ATN, one TMA).

Conclusions: HCT patients exhibit variable biopsy findings, the most common being MGN. Although MGN is frequently observed in allogeneic HCT patients with chronic GVHD, its occurrence after autologous HCT suggests other etiologies. After both auto and allogeneic HCT, MGN may be treated successfully with Rituximab therapy.

1264 Time Dependent Effects of Peroxisome Proliferator-Activated Receptor-γ (PPARγ) Agonist on Acute Puromycin Aminonucleoside (PAN)-Induced Nephrotic Syndrome

Y Zuo, L Ma, AB Fogo. Vanderbilt University, Nashville, TN.

Background: We have previously observed that PPARγ agonists benefit injury in both acute and chronic PAN models, but not if given before PAN. We therefore investigated the mechanisms of time dependence of PPARγ agonist pioglitazone (Pio) effects in PAN nephrotic syndrome.

Design: Adult male SD rats received a single dose of PAN (100mg/kg Bwt, i.p.), and were divided into 4 groups: PAN without further treatment (PAN); Pio (10 mg/kg/d) starting 7 days before PAN (prePio), Pio starting the same day as PAN (Pio0) and Pio starting 4 days after PAN (Piopost). Pio was continued until sacrifice. Serial functional and structural analyses were performed and compared to saline injected rats (N).

Results: Proteinuria (Uprot) increased similarly in all PAN groups by day 4 (PAN 405.8±10.4, prePio 403.9±13.2, Pio0 331.4±69.7, vs N 154.4±12.8 mg/24hr, $P<0.05$). Treatment with Pio at the time of injury or 4 days after significantly reduced day 10 and 21 Uprot (Pio0 605.8±54.2, Piopost 483.3±27.8, vs PAN 758.2±71.6 mg/24hr and Pio0 458.0±78.1, Piopost 474.1±96.4, vs PAN 923.8±93.4 mg/24hr, respectively). By contrast, pretreatment with Pio failed to reduce Uprot either at day 10 or 21 (651.2±50.2 and 729.8±55.6mg/24hr, respectively). Body weight, creatinine clearance (a measure of glomerular filtration rate), plasma volume, and solute-free water clearance rate did not differ among the PAN groups. Pio remarkably decreased the urinary fractional excretion of sodium (Pio0 0.34±0.01, Piopost 0.39±0.05, prePio 0.52±0.02 vs PAN 1.03±0.23% FeNa, $P<0.05$). Potassium excretion also decreased in Pio0 or Piopost but not in prePio (Pio0 26.6±3.7, Piopost 29.7±4.6, prePio 44.9±6.0 vs PAN 44.5±6.2% FeK). Podocyte differentiation, assessed by synaptopodin, was preserved in Pio0 and Piopost, but was remarkably downregulated in prePio. Electron microscopic analysis at day 10 revealed prominent podocyte degeneration with complete foot process effacement (FPE), vacuoles, and microvillous transformation in prePio. In contrast, podocyte injury was less severe in postPio with only subtotal FPE.

Conclusions: Our study shows that PPARγ agonist given simultaneously or even after injury provides time-dependent protective effects against proteinuria in acute nephrotic syndrome without significantly impacting glomerular filtration and fluid excretion. These complex time dependent effects of PPARγ on proteinuria in acute nephrotic syndrome are dependent at least in part on effects on podocyte injury.

Liver & Pancreas

1265 Centrilobular Hepatitis in Pediatric Liver Transplants

SC Abraham, AM Krasinskas, TT Wu. Mayo Clinic, Rochester, MN; Univ of Pittsburgh, Pittsburgh, PA.

Background: Centrilobular hepatitis (CLH) encompasses dropout of zone 3 hepatocytes, red blood cell extravasation, and varying degrees of mononuclear inflammation in the pericentral regions. In the liver transplant (OLT) setting, CLH can occur in isolation or it can occur in association with portal-based disease such as acute rejection (AR). CLH is thought to represent one manifestation of chronic rejection, particularly when accompanied by zone 3 fibrosis. Prior studies of CLH in pediatric liver allografts have been hampered by lack of protocol biopsies and low rates of histologic follow-up.

Design: We studied 58 consecutive liver allografts from 53 pediatric patients (≤18 yrs) who underwent OLT from 1995-2006. All allograft biopsies were scored for the following features: 1) CLH (mild, moderate, severe), 2) portal AR (mild, moderate, severe), 3) zone 3 fibrosis (mild=perivenular or severe=bridging), and 4) ductopenia. Five explanted livers that were removed during the course of retransplantation for graft failure in this group were also reviewed.

Results: Mean age at OLT was 7 yrs (range 7 wks-18 yrs) with 29 boys and 24 girls. We reviewed a total of 417 allograft biopsies (mean 7.2 per allograft) obtained 2 days - 11 yrs post-OLT; 200 (48%) of these were protocol biopsies. Forty-six allografts (79%) had ≥1 yr of histologic follow-up, 29 (50%) had ≥3 yrs, and 21 (36%) ≥5 yrs. Overall, CLH was observed on at least one occasion in 38 (66%) allografts. Of 119 biopsies showing CLH, 70 had CLH + AR, 18 had CLH following an episode of AR within the prior month, 28 had isolated CLH, 3 had CLH + *de-novo* autoimmune hepatitis, and 1 had CLH + EBV infection. Isolated CLH was seen in only 15 (26%) liver allografts; in 2 cases it was due to ischemia or Budd-Chiari syndrome whereas in the other 13 (22%) it appeared to be an immunologic phenomenon. Twenty-four (63%) allografts with CLH developed zone 3 fibrosis (16 mild, 8 severe), 6 (16%) developed ductopenia, and 4 (11%) required retransplant for chronic rejection (n=4). In contrast, only 1 (5%) allograft without CLH developed zone 3 fibrosis (mild; $p<0.0001$) and none developed ductopenia ($p=0.08$) or required retransplant for chronic rejection ($p=0.29$).

Conclusions: CLH is frequent (66%) in pediatric OLT patients. It is most common in association with portal AR or following an episode of portal AR; isolated CLH occurs in only 26% of pediatric liver allografts. CLH is significantly associated with the development of zone 3 fibrosis and there is a trend toward development of ductopenia and need for retransplantation.

1266 Value of Glypican-3 Immunostaining in the Diagnosis of Hepatocellular Carcinoma on Needle Biopsy

F Anatelli, ST Chuang, XJ Yang, HL Wang. Washington University School of Medicine, St. Louis, MO; Northwestern University Feinberg School of Medicine, Chicago, IL.

Background: Histologic diagnosis of hepatocellular carcinoma (HCC) on a needle biopsy can be challenging, particularly in a cirrhotic background. It has been recently reported that glypican-3 (GPC3), a membrane-bound heparan sulfate proteoglycan, is overexpressed in a large proportion of HCCs but undetectable in benign liver tissues. These observations suggest that GPC3 may serve as a very useful biomarker in the diagnosis of difficult HCC cases. However, the diagnostic value of GPC3 immunostaining on needle biopsies has not yet been assessed.

Design: A total of 108 liver needle biopsies were examined in this study. These included 46 cirrhotic livers and 62 HCCs with diagnoses confirmed by subsequent liver resections. Formalin-fixed, paraffin-embedded tissue sections were subjected to immunohistochemical staining using a monoclonal antibody specific for GPC3 (clone 1G12, Biomosaics, Burlington, VT). Positive staining was graded as focal (≤ 50 of the tumor cells stained) or diffuse (>50%).

Results: Strong cytoplasmic and membranous staining for GPC3 was observed in 28 HCCs (45.2%), among which 18 cases (64.3%) showed diffuse immunoreactivity. None of the 46 cirrhotic livers exhibited positive GPC3 immunostaining. The non-neoplastic liver tissues (cirrhotic or non-cirrhotic) that were present in the majority of the HCC cases were also completely negative for GPC3 expression.

Conclusions: GPC3 is a reliable immunohistochemical marker for the diagnosis of HCC on needle biopsies with a high specificity (100%). However, the sensitivity (45%) in our series appears to be lower than that reported in previous studies employing resection specimens as the studying materials. Our findings emphasize the fact that GPC3 immunoreactivity can be focal and that negative staining should not exclude the diagnosis of HCC in challenging needle biopsies.

1267 Reevaluation of "Cancerization of the Duct" by Pancreatic Cancers

S Ban, Y Shimizu, F Ogawa, M Shimizu. Saitama Medical University School of Medicine, Moroyama, Iruma, Saitama, Japan.

Background: Cancerization of the duct (CD) was introduced as one of the mimickers of PaIN in 2001 (Am J Surg Pathol 25:579-586). Afterwards, a consensus meeting of PanIN was held in 2003, and at that meeting two patterns of CD were illustrated by one of the authors of this abstract (MS). At that meeting, CD was defined as a process of secondary involvement of the duct by invasive pancreatic cancer. However, the concept of CD was not totally clarified, especially regarding CD vs. PanIN-3.

Design: Twenty cases of resected pancreatic cancer were evaluated using elastica Masson Goldner stain (EMG) to identify preexisting pancreatic ducts and/or ductules within the area of invasive cancer. Then, the following two patterns of CD were reevaluated. One of the patterns of CD, which is called ductal colonization, and is also known as intraductal spread or intraductal extension, is defined as a direct invasion by invasive cancer cells into the duct continuous to the main lesion. The other CD pattern is ductal invasion, defined as an invasion from the outside of the duct by invasive cancer cells.

Results: Intraductal components (either with papillary structure or with tubular structure) identified by using EMG were often found in the area of invasive cancer. Compared to ductal colonization, luminal obstruction or ductal destruction was more frequently observed in ductal invasion, which was clearly identified by using EMG. In most cases, either ductal colonization or ductal invasion showed similar microscopic findings of the cancer cells between the inside and the outside of the ducts in most cases. Detection of PanIN-3 was very difficult in areas far from the cancerous area.

Conclusions: Recognition of the degree of atypia and the presence of the papillary structure may be helpful to differentiate noninvasive components from invasive components when evaluating the duct by EMG. Luminal obstruction or ductal destruction may favor the diagnosis of ductal invasion. In addition, a mixed pattern comprised of the above-mentioned two patterns may be present.